

Serveur Académique Lausannois SERVAL serval.unil.ch

Author Manuscript

Faculty of Biology and Medicine Publication

This paper has been peer-reviewed but does not include the final publisher proof-corrections or journal pagination.

Published in final edited form as:

Title: Immunosurveillance of lung melanoma metastasis in EBI-3-deficient mice mediated by CD8+ T cells.

Authors: Sauer KA, Maxeiner JH, Karwot R, Scholtes P, Lehr HA, Birkenbach M, Blumberg RS, Finotto S

Journal: Journal of immunology (Baltimore, Md. : 1950)

Year: 2008 Nov 1

Volume: 181

Issue: 9

Pages: 6148-57

In the absence of a copyright statement, users should assume that standard copyright protection applies, unless the article contains an explicit statement to the contrary. In case of doubt, contact the journal publisher to verify the copyright status of an article.

Published in final edited form as:

J Immunol. 2008 November 1; 181(9): 6148–6157.

Immunosurveillance of Lung Melanoma Metastasis in EBI-3-Deficient Mice Mediated by CD8⁺ T Cells¹

Kerstin A. Sauer^{*}, Joachim H. Maxeiner^{2,*}, Roman Karwot^{2,*}, Petra Scholtes^{2,*}, Hans A. Lehr[†], Mark Birkenbach[‡], Richard S. Blumberg[§], and Susetta Finotto^{3,*}

^{*}Laboratory of Cellular and Molecular Immunology of the Lung, I. Medical Clinic, University of Mainz, Germany [†]Institute of Pathology, Centre Hospitalier Universitaire Vaudois, University of Lausanne, Switzerland [‡]Department of Pathology and Department of Anatomy, Eastern Virginia Medical School, Norfolk, VA 23501 [§]Department of Gastroenterology, Brigham and Women's Hospital, Boston, MA 02115

Abstract

EBV-induced gene 3 (EBI-3) codes for a soluble type I receptor homologous to the p40 subunit of IL-12 that is expressed by APCs following activation. In this study, we assessed the role of EBI-3 in a model of lung melanoma metastasis. Intravenous injection of the B16-F10 cell line resulted in a significant reduction of lung tumor metastasis in EBI-3^{-/-} recipient mice compared with wild-type mice. The immunological finding accompanying this effect was the expansion of a newly described cell subset called IFN- γ producing killer dendritic cells associated with CD8⁺ T cell responses in the lung of EBI-3^{-/-} mice including IFN- γ release and TNF- α -induced programmed tumor cell death. Depletion of CD8⁺ T cells as well as targeting T-bet abrogated the protective effects of EBI-3 deficiency on lung melanoma metastases. Finally, adoptive transfer of EBI-3^{-/-} CD8⁺ T cells into tumor bearing wild-type mice inhibited lung metastasis in recipient mice. Taken together, these data demonstrate that targeting EBI-3 leads to a T-bet-mediated antitumor CD8⁺ T cell responses in the lung.

Melanoma is a malignant skin tumor of melanocytic origin that can metastasize to any organ, including the brain and the lung (1).

Cytokines play an important role in controlling tumor growth and metastasis. For instance, IFN- γ is a pleiotropic cytokine whose production relates to Th1 immune responses against pathogens and tumors. IFN- γ production was initially associated with cells of lymphoid origin, particularly NK and T cells (2, 3). It is now, however, clear that cells of the myeloid

¹This work was supported by the Graduiertenkolleg 1043 (Antigenspezifische Immuntherapie) and the ICE-Immunology Cluster of Excellence-Immunointervention.

© 2008 by The American Association of Immunologists, Inc.

³Address correspondence and reprint requests to Prof. Susetta Finotto, Laboratory of Cellular and Molecular Lung Immunology, I. Medical Clinic, University of Mainz, Obere Zahlbacher Strasse 63, Room 2-110, Mainz, Germany. finotto@mail.uni-mainz.de.

²J.H.M., R.K., and P.S. contributed equally to this work.

Disclosures

Susetta Finotto has a patent together with the University of Mainz on EBI-3. Patent No. WO/2007/045389.

lineage dendritic cells (DCs)⁴ and macrophages are also capable to produce this cytokine. Specifically, a novel cell subset denoted IFN- γ producing killer DCs (IK-DCs), with cross-priming functions has been recently described to express markers related to those of plasmacytoid DCs and NK cells. It has been suggested that this cell population might function as a tumor scavenger by producing high amounts of IFN- γ (4 – 6).

The EBV induced gene 3 (EBI-3) can associate with p28 to form the cytokine IL-27. IL-27 (EBI-3-p28) is known to be an early product of activated APCs that is produced upon TLR ligation. It drives a rapid clonal expansion of naive but not memory CD4⁺ T cells, and synergizes with IL-12 to trigger IFN- γ production via T-bet from naive splenic CD4⁺ T cells (7). A distinct receptor for IL-27 consists of the orphan receptor WSX-1/TCCR, a novel class I cytokine receptor with homology to the IL-12 receptors, highly expressed in lymphoid tissue and associates with gp130 (8). IL-27 induces expression of T-bet and IL-12R β 2 through WSX-1 signaling in wild-type naive CD4⁺ T cells indicating that IL-27/WSX-1 signaling is important for the initial commitment of Th1 responses (9).

Although IL-27 has been shown to positively regulate Th1 pathways, EBI-3 could have additional functions in T cell differentiation and activation that remain to be investigated. In this regard, it has been recently shown that EBI-3 can also associate with the p35 unit of IL-12 to form a new cytokine denoted as IL-35 (EBI-3-p35 heterodimer). IL-35 contributes to the suppressive function of regulatory CD4⁺CD25⁺Foxp-3⁺ T cells known to suppress antitumoral immunity (10). Moreover, experimental evidences suggest a role of EBI-3 independent from p28, as many tumors are characterized by the selective expression of EBI-3 in the absence of p28 (11, 12).

In the current manuscript, we demonstrate that targeted deletion of EBI-3 protected mice from lung metastasis upon i.v. injection of the transformed cell line B16-F10. We further demonstrate that EBI-3 deficiency induced CD11c⁺B220⁺NK1.1⁺Gr1⁻ (IFN- γ -releasing) cells in the lung which was associated with increased local CD8⁺ T cell antitumor responses. Finally, targeted deletion of T-bet resulted in increased tumor load in EBI-3-deficient mice indicating that T-bet is involved in the EBI-3^{-/-} protection from melanoma metastasis. These results indicate a novel role of EBI-3 in controlling tumor metastasis via lung CD8⁺ T cells and suggest that targeted deletion of EBI-3 could be beneficial for therapy of lung melanoma metastasis.

Materials and Methods

Mice

C57BL/6 mice were obtained from Charles River Laboratories and The Jackson Laboratory. EBI-3^{-/-} have been described previously (13) and were on a pure C57BL/6 genetic background. T-bet^{-/-} mice were gift from Professor L.H. Glimcher (Harvard Medical School, Boston, MA) and were also on a C57BL/6 genetic background (14). EBI-3^{-/-} and T-bet^{-/-} mice were backcrossed for at least ten generations on a C57BL/6 genetic

⁴Abbreviations used in this paper: DC, dendritic cell; IK-DC, IFN- γ producing killer DC; EBI-3, EBV induced gene 3; BALF, bronchoalveolar lavage fluid; pDC, plasmacytoid dendritic cell.

background before entering the experiments described in this manuscript. Animals were bred and maintained under specific pathogen-free conditions in our animal facility and treated according to institutional animal care guidelines.

Tumor cell injection

B16-F10 melanoma cells were kindly given to us by Prof. Laurie H. Glimcher (Harvard Medical School, Boston, MA) and cultured in DMEM enriched with 10% FCS (Biofluids) and antibiotics. The cell line was tested negative for mycoplasma and other transmissible infectious agents. A total of 2×10^5 cells resuspended in 0.2 ml sterofundin (Braun) were injected into the lateral tail vein. At the indicated following days lungs were removed, placed in medium, and microscopically analyzed as reported below.

In additional experiments, CD8⁺ and NK1.1⁺ T cells were targeted by five i.p. applications of anti CD8 (Hybridoma 53.6.72, gift from Dr Stephan Sudowe, Dermatology Department, University of Mainz, Germany) (250 µg/200 µl) and anti-mouse NK1.1 (Ly-55; eBioscience) (100 µg/200 µl) Abs at days 4, 7, 11, 14, and 17 after tumor cell injection. These treatments led to complete depletion of CD8⁺ T cells and a 50% reduction of the NK1.1⁺ cells, respectively.

Quantification of lung metastasis

Lungs were removed and metastases were photographed under the stereo microscope Stemi 200-C with an AxioCam MRc. The pictures were imported on a computer by Axiovision 4.2. from Carl Zeiss Vision GmbH and metastases were marked both on the front and back side pictures of each lung. The total area occupied by the melanin-rich colonies was analyzed. The total melanotic area was compared with the size of the whole lung by using an Excel computer program. Results are shown as percentages.

Collection and analysis of the bronchoalveolar lavage fluid (BALF)

BALF of the right lung was collected as described previously (15).

Histological analysis of tumor mass

For histological analysis, lung samples were immersed in 10% buffered formalin before embedding in paraffin, sectioned, stained, and quantified by the Pathological Department at the University of Lausanne, Switzerland and imported in Photoshop (Adobe Systems, Version 7.0) as previously described (16). Space bars correspond to 2.5 mm for the histological overviews and 200 µm for the high magnification images.

Isolation and analysis of total lung CD11c⁺ and CD8⁺ T cells

Total lung cell suspension was obtained as previously described (17). The CD11c⁺ and CD8⁺ lung cells were directly purified from isolated lung cell suspension according to the manufacturer's instructions and as previously described (18, 19). After three washes in complete medium, the CD11c⁺ cells were cultured with LPS (*Escherichia coli* 0111:B4 LPS, 1 µg/ml; InvivoGen) for 24 h at a density of 10^6 cells/ml. Spleen CD11c⁺ cells were cultured in RPMI 1640 culture medium enriched with 5% FBS alone or with LPS (1 mg/ml)

and CpG (CpG-ODN-1826-5'-t(PTO)CC-ATG-ACG-TTC-CTG-ACG-t(PTO)t(PTO)-3') or GpC (GpC-ODN1745-5'-t(PTO)-CC-ATG-ACG-TTC-CTG-AGC-t(PTO)t(PTO)-3'), 10 μ M each (Bio-Spring).

After three washes in complete medium, the CD8⁺ T cells were cultured with plate-bound anti-CD3 Abs (CD3 clone 145-2C11, 5 μ g/ml; BD Pharmingen) for 24 h at a density of 10⁶ cells/ml. Supernatants were analyzed for cytokine production by ELISA. Alternatively, CD8⁺ T cells were cocultured with B16-F10 cells and different concentrations of anti-TNF- α Abs (R&D Systems).

Twenty four hours later, cell pellets were processed for cell apoptosis in accordance to the Annexin-V-propidium iodide staining (Annexin V-FITC apoptosis detection kit II; BD Pharmingen). Cells were washed in cold PBS and resuspended in binding buffer. In brief, 10⁵ cells were then incubated with Annexin V-FITC and propidium iodide and analyzed within 1 h by FACS analysis in accordance to the manufacturer's instructions.

As positive control, the B16-F10 melanoma cell line was incubated with different concentrations of recombinant mouse TNF- α (eBioscience, Natu-Tec) and apoptosis was measured 24 h later as indicated above.

FACS analysis

To assure the purity of isolated cells, routinely, 1 \times 10⁵ cells were washed with 1 ml PBS and then incubated for 30 min in 100 μ l PBS containing 5 μ g/ml of anti-mouse CD8-allophycocyanin (53-6.7-allophycocyanin) (BD Pharmingen) or anti-mouse CD11c-FITC (BD Pharmingen). Cells were washed with 1 ml of PBS. Resulting cell suspensions were measured by FACSCalibur and analyzed by using Cell Quest Pro version 4.02 (BD Pharmingen).

Total lung cells were stained with FACS Abs and analyzed as described above.

The following Abs were used: anti-mouse CD8 α (53-6.7-allophycocyanin) Ab (BD Pharmingen), anti-mouse CD69 (H1.2F3 FITC) Ab (BD Pharmingen), anti-mouse CD44 (Pgp-1, Ly-24 PE Cy5) Ab (BD Pharmingen), anti-mouse CD11c-FITC (BD Pharmingen), anti-mouse CD45R-PE-Cy5.5 Ab (eBioscience), anti-mouse PDCA-1-PE Ab (Miltenyi Biotec), anti-mouse NK1.1-allophycocyanin Ab (Caltag Laboratories), anti-mouse CD49d-PE Ab (eBioscience), anti-mouse CD122 (TM- β 1-PE) Ab (BD Pharmingen), Annexin V-FITC (BD Pharmingen), propidium iodide (BD Pharmingen), anti-mouse CD11c-allophycocyanin Ab (eBioscience), and anti-mouse Gr1(Ly6c)-PE (eBioscience).

Intracellular cytokine analysis

For intracellular staining of IFN- γ , isolated lung CD11c⁺ cells were cultured overnight with LPS (1 μ g/ml) and CpG-DNA (10 pmol/ml) and then stimulated with 1 ng/ml PMA (Sigma-Aldrich), 1 μ mol ionomycin, LPS (1 μ g/ml), and GolgiStop (BD Pharmingen) for 4 h at 37°C. Cells were stained with anti-mouse CD8 α (53-6.7- PE) (BD Pharmingen), anti-mouse CD45R-PE-Cy5.5 Ab (eBioscience), and anti-mouse NK1.1-allophycocyanin Ab (Caltag Laboratories) Abs for 30 min at 4°C. Thereafter, cells were fixed with PBS containing 2%

(v/v) paraformaldehyde for 15 min at room temperature and washed twice with PBS and once with PBS containing 0.1% (weight-to-volume ratio) saponin, 0.5% BSA, and 0.01% NaN₃ (permeabilization fluid). Cells were then incubated with FITC-labeled Abs against IFN- γ (XMG 1.2- PE) (BD Pharmingen) for 30 min at 4°C in permeabilization fluid and washed twice.

ELISA

IL-12p70 was detected in the bronchoalveolar lavage fluid by using a mouse-specific ELISA Set (OptEIA, Standard range from 62.5 to 4000 pg/ml, BD Pharmingen). IL-12p40 was detected in cell supernatants using a mouse-specific ELISA Set (OptEIA, Standard range from 15.625 to 1000 pg/ml, BD Pharmingen). The IFN- γ -ELISA was performed from BALF and cell supernatants using a sandwich ELISA Set (OptEIA, Standard range from 31.3 to 2000 pg/ml, BD Pharmingen). TNF- α was detected in BALF and cell supernatants using a specific sandwich ELISA Set (OptEIA; Standard range from 15.6 to 1000 pg/ml; BD Pharmingen).

Statistical analysis

Differences were evaluated for significance ($p < 0.05$) by the Student's two-tailed t test for independent events (Excel, PC). The coefficient of correlations was calculated by using the statistical analysis of the Excel program. Data are given as mean values \pm SEM.

Results

EBI-3 deficiency protects mice from metastases of lung melanoma

To analyze the role of EBI-3 in lung metastasis, we studied the lung melanoma development in EBI-3-deficient mice (9) and wild-type mice after i.v. injection of B16-F10 cells. It was found that targeted deletion of EBI-3 results in increased survival of mice bearing lung melanoma compared with wild-type littermates. Specifically, a dramatic drop in the survival rate of wild-type mice started at day 21 after i.v. injection of B16-F10 (Fig. 1a), whereas 100% of the EBI-3-deficient mice survived until day 28 (at which time 50% of the wild-type mice bearing tumor were already dead). At day 33, 100% of the wild-type mice bearing tumor were dead, whereas 50% of EBI-3-deficient mice were still alive (Fig. 1a). To monitor the development of the lung melanoma, we microscopically analyzed and counted lung colony formation, by means of a stereomicroscope at different time points both in wild-type and EBI-3^{-/-} B16-F10 cell injected mice, as shown in Fig. 1b. Starting at day 10, a significant increase in lung melanotic colonies could be appreciated in the wild-type mice compared with EBI-3^{-/-} B16-F10 cell injected mice (Fig. 1b, *upper and lower rows*, respectively). This difference was maintained until day 21 when the wild-type mice started to die (Fig. 1a).

In addition, the same results were found after histological quantification of the metastatic colonies, where tumor cells were visible as brown spotted cells after H&E staining (Fig. 2). Notably, an increased number of cells per colony were found on the surface of the lungs of wild-type littermates at day 10, indicating an early colonization on the surface of the lung as compared with deeper areas of the parenchyma. In fact, the brown tumor cells could be

followed histologically from the vessels to the pleura (Fig. 2*b*, *left panels*). In contrast to wild-type mice, 5 days after tumor cell transfer, no tumor colonies were seen at the surface of the lungs of EBI-3^{-/-} mice and only few small colonies (Fig. 2, *a* and *b*) were noted histologically in the deeper areas of the lung.

Increased IL-12p70 levels in the airways of EBI-3^{-/-} mice developing lung melanoma

IL-12 is a cytokine released during the innate immune response that can induce T cell effector functions. We next analyzed IL-12p70 levels in the BALF of wild-type and EBI-3^{-/-} mice developing metastases upon B16-F10 injection. As shown in Fig. 3*a* (*left panel*), we detected increased levels of IL-12p70 in the BALF of EBI-3^{-/-} mice compared with wild-type litter-mates at day 10 after B16-F10 injection. It is thus possible that in the absence of IL-27, a compensatory increased release of IL-12 takes place in the lung of EBI-3-deficient mice (17). IL-12 is produced by DCs and NK cells. We thus isolated lung CD11c⁺ cells and measured IL-12p40 in the cell supernatant. As shown in Fig. 3*a* (*right panel*), increased levels of IL-12p40 were detected in the supernatants of lung CD11c⁺ cells isolated from the EBI-3^{-/-} mice at day 10. This cytokine was also released at high concentrations at day 5 both in wild-type and EBI-3^{-/-} mice, although no differences between both groups were noted at that time point (data not shown).

Increased number of CD11c⁺NK1.1⁺ B220⁺Gr1⁻(Ly6c⁻) cells in the lungs of EBI-3-deficient mice

The differences in IL-12 levels were detected at day 10 when histopathological differences were already macroscopically visible between wild-type and EBI-3^{-/-} mice (Fig. 1*b*). We thus investigated earlier changes in immune responses in the lung of EBI-3^{-/-} mice.

B220⁺CD11c⁺NK1.1⁺Gr1⁻ cells have the capacity to present Ag after activation of TLR-9 and may be involved in tumor Ag cross presentation to T cells (20–25). To test whether B220⁺CD11c⁺NK1.1⁺ cells might play a role in controlling lung metastasis in our model, we next analyzed DCs isolated from the lungs of wild-type and EBI-3-deficient mice, before (day 0) and 5 days (Day 5) after i.v. injection of B16-F10 cells. Classical plasmacytoid dendritic cells (pDCs) expressing CD11c, B220, PDCA-1, and Gr1 (Ly6c) were increased in the lungs of EBI-3^{-/-} mice bearing metastases 5 days after the i.v. injection of B16-F10 (Fig. 3*b*, *upper and middle panels*) as compared with wild-type littermates. We then focused on the characterization of CD11c⁺B220⁺NK1.1⁺Gr1⁻ cells that display both plasmacytoid and cell killer features (26). These CD11c⁺ or CD11c^{int} express both B220 (CD45R) and NK1.1 but are Gr1⁻. We found that the number of CD11c⁺B220⁺NK1.1⁺ cells represents around 50% of lung CD11c⁺ cells in both untreated and tumor-bearing EBI-3^(-/-) mice and that the number of these cells is increased in EBI-3-deficient mice as compared with wild-type mice (Fig. 3*b*, *lower panel*). Therefore, B220⁺CD11c⁺NK1.1⁺ cells represent the vast majority of the CD11c cells populating the lung of EBI-3^{-/-} mice at day 5.

As B220⁺CD11c⁺NK1.1⁺ cells are known to produce IFN- γ , we next analyzed IFN- γ production by isolated CD11c⁺ cells after overnight culture and found that these cells isolated from the lungs of tumor bearing EBI-3^{-/-} mice (day 5 after the i.v. injection of B16-F10 cells) released significantly higher amounts of IFN- γ as compared with those isolated

from the wild-type littermates (Fig. 3c, upper left panel). The IFN- γ production by lung B220⁺CD11c⁺NK1.1⁺ cells was further confirmed by intracellular staining with anti-IFN- γ Abs on purified lung CD11c⁺ cells by gating on CD45R⁺NK1.1⁺ cells (Fig. 3c, lower panels).

Moreover, consistent with the increased presence of the B220⁺CD11c⁺NK1.1⁺ cell phenotype in the lung, splenocytes taken from EBI-3^(-/-) mice released increased amounts of IFN- λ upon challenge with LPS and CpG as compared with those obtained from the wild-type littermates that were challenged under the same conditions (Fig. 3c, upper right panel). These findings altogether suggested that the antitumor function of B220⁺CD11c⁺NK1.1⁺ cells in this model may relate to IFN- γ production.

Expansion of activated CD8⁺ T cells releasing IFN- γ in the lungs of EBI-3-deficient mice in a murine model of melanoma

IFN- γ secretion plays an important role during both innate and acquired immunity by enhancing Th1-type immune responses. This cytokine is produced by multiple cell types and CD8⁺ T cells are a potential main source of IFN- γ production in vivo. To start to analyze this possibility, we isolated and characterized CD8⁺ T cells from the lungs of wild-type and EBI-3^(-/-) mice upon injection of B16-F10 cells.

CD8⁺ T (CD8⁺CD44⁺CD49d⁺) cells expressing markers of cell adhesion and activation were increased in the lungs of the EBI-3^(-/-) mice as compared with wild-type mice (Fig. 4b, upper panels). Interestingly, the CD8⁺CD122⁺ population, which is known to down-regulate IFN- γ production and proliferation (26, 27), was found to be decreased in the lungs of EBI-3^(-/-) mice 5 days after tumor cell injection (Fig. 4b, lower panels). Consistently, at the same time point, lung CD8⁺ T cells from EBI-3^(-/-) mice produced significantly higher levels of IFN- γ as compared with wild-type controls (Fig. 4a). Furthermore, a significant increase in the number of CD8⁺ T cells in the lung of EBI-3^(-/-) mice was observed as compared with EBI-3^(-/-) mice. Whereas an expansion of CD8⁺ T cells was noted in EBI-3^(-/-) mice during tumor development, the CD8⁺ T cells seems to be constant as the tumor developed in the wild-type littermates, suggesting a stronger CD8⁺ T cells antitumor Ag response in the lung of EBI-3^(-/-) mice (Fig. 4c).

Apoptosis of B16-F10 cells is induced in vivo by TNF- α released by CD8⁺ T cells isolated from the lungs of EBI-3-deficient mice

We then asked the question whether injected B16-F10 cells were not able to cause large lung metastases in EBI-3^(-/-) lungs because of increased cytotoxicity induced by CD8⁺ T cells. As IFN- γ is known to synergize with TNF- α to induce cell death, we analyzed in situ apoptosis of tumor cells once they reached the lung. We found increased cell apoptosis in large size lung cells isolated from EBI-3-deficient mice, as compared with those obtained from the wild-type littermates 10 days after i.v. injection of B16-F10 cells (Fig. 5a). These findings indicated an increased tumor cell killing capacity in the cellular component isolated from the lungs of EBI-3-deficient mice as compared with wild-type littermates at a later time point after IFN- γ release. Accordingly, we next focused on lung CD8⁺ T cells and found that lung CD8⁺ T cells released increased TNF- α levels when isolated from EBI-3^(-/-) mice at days 5

and 10 (Fig. 5b) after tumor cell injection as compared with wild-type mice. TNF- α is known to induce programmed cell death via TNF receptor signaling. Neutralization of TNF- α with increasing concentrations of an anti-TNF- α Ab was then performed in cell coculture experiments in which CD8⁺ T cells were isolated from the lungs of EBI-3^{-/-} mice at different time points after i.v. injection of B16-F10 and cocultured with B16-F10 cells. As shown in Fig. 5c, apoptosis of B16-F10 cells could be neutralized with anti-TNF- α Abs in a dose-dependent manner when CD8⁺ T cells were isolated 5 days after tumor cell injection and cocultured with B16-F10 cells (1:1 ratio). The sensitivity of B16-F10 to TNF- α induced apoptosis is also reported as positive control in Fig. 5d. As shown, increasing doses of TNF- α induced the number of Annexin V-positive B16-F10 cells significantly.

Targeted deletion of T-bet abrogated the protective effect of EBI-3 deficiency on melanoma metastases

To demonstrate that IFN- γ released by CD8⁺ T cells as well as by NK cells plays a central role in the protection of lung melanoma development in EBI-3^{-/-} mice, we next performed depletion experiments as specified in *Materials and Methods*. Five i.p. applications of anti CD8 Abs (250 μ g/200 μ l) led to complete depletion of the CD8⁺ T cells in EBI-3^{-/-} mice, as shown in Fig. 6b by dot plot analysis. The depletion of CD8⁺ T cells resulted in an induction of the tumor load in EBI-3^{-/-} mice as shown in Fig. 6a, on the left hand side and as quantified on the right panel. These results demonstrate that in the absence of EBI-3, which is expressed by APCs, CD8⁺ T cells mediate increased protection against metastases. Furthermore, we show that both depletion of CD8⁺ and decrease of NK1.1⁺ cells in EBI-3-deficient mice bearing tumors, resulted in significant decrease in IFN- γ production in total lung cells after intracellular staining (Fig. 6d) as compared with untreated mice. These data indicate that CD8⁺ and NK1.1⁺ cells are the major source of IFN- γ (Fig. 6d) in EBI-3 deficient mice. We then looked at IFN- γ release in the BALF of anti CD8 and anti NK1.1 Abs treated mice and found, as shown in Fig. 6f, that depletion of CD8 resulted in a stronger inhibition of IFN- γ release in the airways as compared with anti NK1.1 in EBI-3^{-/-} mice. Thus, the observed protection from lung melanoma in EBI-3^{-/-} mice is dependent on the increase IFN- γ production mainly by CD8⁺ T cells. Moreover, we could demonstrate after intracellular staining for IFN- γ on total lung cells and gating on CD8⁺ T cells (Fig. 6e), that depletion of NK1.1 positive cells by anti NK1.1 Abs led to a 50% decrease of INF- γ production by CD8⁺ T cells indicating that CD8⁺ T cells release the effectors cytokine IFN- γ also in a NK1.1 dependent manner.

Noteworthy was the observation that the anti NK1.1 Ab-induced partial depletion was not accompanied by increased tumor load in treated mice (Fig. 6a). Furthermore, we did not observe any significant decrease in IL-12p70 and IL-12p40 production after anti NK1.1. and anti CD8 Ab treatment.

We thus concluded that the observed protected phenotype observed in EBI-3^{-/-} mice was dependent on the total IFN- γ production in these mice with CD8⁺ T cell being the major source of this cytokine.

To definitively show the dependency on IFN- γ on the protective phenotype observed in EBI-3^{-/-} mice, and considering that T-bet^{-/-} mice are defective in NK cells, we crossed

EBI-3^{-/-} mice with T-bet^{-/-} mice. The resulting double KO mice showed a significant increase in the number and size of the metastatic colonies providing striking evidence that T-bet and therefore IFN- γ are involved in EBI-3-induced melanoma (Fig. 6c). As shown, this effect was dose-dependent as indicated by the intermediate tumor load shown by the EBI-3^{-/-}T-bet^{-/-} mice (Fig. 6c, *middle panel*).

In vivo transfer of CD8⁺ T cells isolated from EBI-3-deficient mice bearing tumor protects wild-type recipient mice from B16-F10-induced lung tumors

To directly prove the in vivo relationship between lung tumor size and the apoptotic function of CD8⁺ T cells isolated from the EBI-3-deficient mice, we adoptively transferred these CD8⁺ T cells together with B16-F10 cells i.v. into wild-type mice. To perform this experiment, CD8⁺ T cells were isolated from the lungs of EBI-3-deficient and wild-type mice 5 days after tumor cell injection when the IFN- γ production by CD8⁺ T cells isolated from the EBI-3^{-/-} lungs was significantly increased compared with IFN- γ released by the wild-type CD8⁺ T cells. As shown in Fig. 7a, wild-type mice could be rescued from the development of lung metastases upon i.v. administration of CD8⁺ T cells isolated from EBI-3-deficient (but not wild-type) mice that had been injected with the tumor cell line 5 days before. This macroscopic finding was accompanied by an increased number of activated CD8⁺ T cells (Fig. 7b). Furthermore, activated CD8⁺ T cells produced elevated levels of TNF- α in the BALF of mice given activated EBI-3^{-/-} CD8⁺ T cells (Fig. 7c).

Discussion

In this manuscript, we report that targeted deletion of EBI-3 increases the survival of mice developing lung melanoma. In addition, we started to elucidate the immunological mechanism that allowed EBI-3-deficient mice to escape from tumor metastases. In fact, we reported in this study that, in the absence of EBI-3, lung CD11c⁺ cells expressed increased markers of a newly described cell subset known as IK-DC that produces IFN- γ . This is a distinct population of cells that expresses similar levels of CD11c, B220, and MHC II as pDCs, but has markers reminiscent of NK cells as well (6, 24). This cell subset has been further characterized recently as a discrete NK cell subset capable of producing higher levels of IFN- γ than conventional NK cells (20, 21, 23). Moreover, we demonstrated that IK-DCs/B220⁺CD11c⁺NK1.1⁺Gr1⁻ cells are increased in the lungs of EBI-3^{-/-} mice and released increased amounts of IFN- γ .

NK cells are known to exhibit reciprocal-activating interactions with DCs (22, 26). We recently found that IK-DCs develop preferentially in the lungs and not in the adjacent lymph nodes (K. A. Sauer and S. Finotto, unpublished data). In fact, IK-DCs represent up to 50% of the local CD11c⁺ cells in the normal murine lung indicating a potential regulatory role of these cells in an anatomical location where lung metastasis is initiated. In the present study, we have shown that IK-DCs are expanded in the lungs of EBI-3-deficient mice in an experimental model of lung metastasis as compared with control mice. Moreover, these EBI-3^{-/-} IK-DCs produced increased amounts of IFN- γ as compared with control cells from wild-type mice.

In the presence of IL-12 and IFN- γ , CD8⁺ T cells may polarize into IFN- γ -producing cells and promote the differentiation of T cells into killer cells releasing TNF- α (28–31). As IFN- γ is instrumental for enhancing Ag processing and presentation for optimal recognition of tumor cells by T cells, the increased levels of IFN- γ produced by lung IK-DCs could contribute to CD8⁺ T cell differentiation and activation in EBI-3-deficient mice. Consistent with this hypothesis, EBI-3^{-/-} CD8⁺ T cells isolated from the lungs of EBI-3^{-/-} mice 5 days after i.v. injection of B16-F10 cells induced cell death of B16-F10 cells ex vivo. Furthermore, these EBI-3^{-/-}CD8⁺ T cells produced increased amounts of TNF- α and neutralization of TNF- α ex vivo reduced the CD8⁺ T cell induced apoptosis in B16-F10 cells demonstrating that EBI-3^{-/-} CD8⁺ T cells utilize TNF- α to kill the tumor. The functional relevance of the latter cells in vivo could be demonstrated using adoptive transfer studies in which transfer of EBI-3^{-/-} CD8⁺ T cells led to significantly stronger reduction of developing tumors in B16-F10 injected wild-type littermates as compared with the transfer of wild-type cells. Consistently, targeting CD8⁺ T cells by using neutralizing Abs resulted in an increased tumor area in EBI-3^{-/-} mice.

These data show for the first time an effect of EBI-3 on CD8⁺ T cells. In the absence of EBI-3, these cells produced significantly higher amounts of IFN- γ than wild-type cells. As all currently known cytokines involving EBI-3 are known to induce rather than reduce IFN- γ production by T cells (9), it is tempting to speculate that this function of EBI-3 could be due to currently unrecognized binding partners for EBI-3. By crossing EBI-3^{-/-} mice with T-bet^{-/-} mice, we definitively proved a direct function of EBI-3 on T-bet and IFN- γ independently from IL-27. In fact, the double-deficient mouse (EBI-3^{-/-}T-bet^{-/-} mouse) showed increased tumor load in a dose-dependent manner as indicated by the intermediate tumor load shown by the EBI-3^{-/-}T-bet^{+/-} mice.

IFN- γ can inhibit the growth of tumor cells as well as promote the production of other type I cytokine and differentiation of cytotoxic NK and T cells (32). T-bet-deficient mice have impaired CTL responses to Ag (33) and adoptive transfer of wild-type-activated NK cells protects T-bet^{-/-} mice after melanoma challenge showing that reconstitution of the NK compartment in these mice is sufficient to mediate a significant reduction of the tumor burden (14). In fact, T-bet-deficient mice have increased metastases load accompanied by reduced number of NK cells and no NKT cells infiltrating tumor-bearing tissue in this model, thus providing an appropriate genetic background on the role of NK cells in EBI-3-deficient mice (14). Consistently, we previously reported increased T-bet in the lung of EBI-3^{-/-} mice in a murine model of asthma (18). Taken together, these results suggest a role of T-bet in EBI-3^{-/-}-mediated melanoma protection, confirming a role of IFN- γ in our findings and providing a linkage between innate and adaptive immune-response in tumor.

Our findings are the first demonstration that activation of the antitumor immune response in the lungs is orchestrated by increased B220⁺CD11c⁺NK1.1⁺ cells that modulate local CD8⁺ T cell responses in the absence of EBI-3.

These results have important implications for new therapies aiming at the cure of metastatic diseases such as lung melanoma.

Acknowledgments

The authors thank Isabel Ernst for excellent technical help.

References

1. Gray-Schopfer V, Wellbrock C, Marais R. Melanoma biology and new targeted therapy. *Nature*. 2007; 445:851–857. [PubMed: 17314971]
2. Neurath MF, Finotto S, Glimcher LH. The role of Th1/Th2 polarization in mucosal immunity. *Nat Med*. 2002; 8:567–573. [PubMed: 12042806]
3. Szabo SJ, Sullivan BM, Stemmann C, Satoskar AR, Sleckman BP, Glimcher LH. Distinct effects of T-bet in TH1 lineage commitment and IFN- γ production in CD4 and CD8 T cells. *Science*. 2002; 295:338–342. [PubMed: 11786644]
4. Chan CW, Crafton E, Fan HN, Flook J, Yoshimura K, Skarica M, Brockstedt D, Dubensky TW, Stins MF, Lanier LL, et al. Interferon-producing killer dendritic cells provide a link between innate and adaptive immunity. *Nat Med*. 2006; 12:207–213. [PubMed: 16444266]
5. Taieb J, Chaput N, Menard C, Apetoh L, Ullrich E, Bonmort M, Pequignot M, Casares N, Terme M, Flament C, et al. A novel dendritic cell subset involved in tumor immunosurveillance. *Nat Med*. 2006; 12:214–219. [PubMed: 16444265]
6. Ullrich E, Bonmort M, Mignot G, Chaput N, Taieb J, Menard C, Viaud S, Tursz T, Kroemer G, Zitvogel L. Therapy-induced tumor immunosurveillance involves IFN-producing killer dendritic cells. *Cancer Res*. 2007; 67:851–853. [PubMed: 17283111]
7. Brombacher F, Kastelein RA, Alber G. Novel IL-12 family members shed light on the orchestration of Th1 responses. *Trends Immunol*. 2003; 24:207–212. [PubMed: 12697453]
8. Yoshida H, Hamano S, Senaldi G, Covey T, Faggioni R, Mu S, Xia M, Wakeham AC, Nishina H, Potter J, et al. WSX-1 is required for the initiation of Th1 responses and resistance to *L. major* infection. *Immunity*. 2001; 15:569–578. [PubMed: 11672539]
9. Takeda A, Hamano S, Yamanaka A, Hanada T, Ishibashi T, Mak TW, Yoshimura A, Yoshida H. Cutting edge: role of IL-27/WSX-1 signaling for induction of T-bet through activation of STAT1 during initial Th1 commitment. *J Immunol*. 2003; 170:4886–4890. [PubMed: 12734330]
10. Collison LW, Workman CJ, Kuo TT, Boyd K, Wang Y, Vignali KM, Cross R, Sehy D, Blumberg RS, Vignali DA. The inhibitory cytokine IL-35 contributes to regulatory T-cell function. *Nature*. 2007; 450:566–569. [PubMed: 18033300]
11. Larousserie F, Bardel E, Pflanz S, Arnulf B, Lome-Maldonado C, Hermine O, Bregeaud L, Perennec M, Brousse N, Kastelein R, Devergne O. Analysis of interleukin-27 (EBI3/p28) expression in Epstein-Barr virus- and human T-cell leukemia virus type 1-associated lymphomas: heterogeneous expression of EBI3 subunit by tumoral cells. *Am J Pathol*. 2005; 166:1217–1228. [PubMed: 15793300]
12. Larousserie F, Bardel E, Coulomb L'Hermine A, Canioni D, Brousse N, Kastelein RA, Devergne O. Variable expression of Epstein-Barr virus-induced gene 3 during normal B-cell differentiation and among B-cell lymphomas. *J Pathol*. 2006; 209:360–368. [PubMed: 16639698]
13. Wirtz S, Tubbe I, Galle PR, Schild HJ, Birkenbach M, Blumberg RS, Neurath MF. Protection from lethal septic peritonitis by neutralizing the biological function of interleukin 27. *J Exp Med*. 2006; 203:1875–1881. [PubMed: 16880260]
14. Werneck MB, Lugo-Villarino G, Hwang ES, Cantor H, Glimcher LH. T-bet plays a key role in NK-mediated control of melanoma metastatic disease. *J Immunol*. 2008; 180:8004–8010. [PubMed: 18523263]
15. Maxeiner JH, Karwot R, Hausding M, Sauer KA, Scholtes P, Finotto S. A method to enable the investigation of murine bronchial immune cells, their cytokines and mediators. *Nat Protoc*. 2007; 2:105–112. [PubMed: 17401344]
16. Doganci A, Eigenbrod T, Krug N, De Sanctis GT, Hausding M, Erpenbeck VJ, Haddad EB, Lehr HA, Schmitt E, Bopp T, et al. The IL-6R α chain controls lung CD4⁺CD25⁺ Treg development and function during allergic airway inflammation in vivo. *J Clin Invest*. 2005; 115:313–325. [PubMed: 15668741]

17. Sauer KA, Scholtes P, Karwot R, Finotto S. Isolation of CD4⁺ T cells from murine lungs: a method to analyze ongoing immune responses in the lung. *Nat Protoc.* 2006; 1:2870–2875. [PubMed: 17406546]
18. Hausding M, Karwot R, Scholtes P, Lehr HA, Wegmann M, Renz H, Galle PR, Birkenbach M, Neurath MF, Blumberg RS, Finotto S. Lung CD11c⁺ cells from mice deficient in Epstein-Barr virus-induced gene 3 (EBI-3) prevent airway hyper-responsiveness in experimental asthma. *Eur J Immunol.* 2007; 37:1663–1677. [PubMed: 17506035]
19. Karwot R, Maxeiner JH, Schmitt S, Scholtes P, Hausding M, Lehr HA, Glimcher LH, Finotto S. Protective role of nuclear factor of activated T cells 2 in CD8⁺ long-lived memory T cells in an allergy model. *J Allergy Clin Immunol.* 2008; 121:992–999.e6. [PubMed: 18329088]
20. Allan RS, Smith CM, Belz GT, van Lint AL, Wakim LM, Heath WR, Carbone FR. Epidermal viral immunity induced by CD8 α ⁺ dendritic cells but not by Langerhans cells. *Science.* 2003; 301:1925–1928. [PubMed: 14512632]
21. Banchereau J, Steinman RM. Dendritic cells and the control of immunity. *Nature.* 1998; 392:245–252. [PubMed: 9521319]
22. Belz GT, Smith CM, Kleinert L, Reading P, Brooks A, Shortman K, Carbone FR, Heath WR. Distinct migrating and nonmigrating dendritic cell populations are involved in MHC class I-restricted antigen presentation after lung infection with virus. *Proc Natl Acad Sci USA.* 2004; 101:8670–8675. [PubMed: 15163797]
23. Heath WR, Belz GT, Behrens GM, Smith CM, Forehan SP, Parish IA, Davey GM, Wilson NS, Carbone FR, Villadangos JA. Cross-presentation, dendritic cell subsets, and the generation of immunity to cellular antigens. *Immunol Rev.* 2004; 199:9–26. [PubMed: 15233723]
24. Shortman K, Villadangos JA. Is it a DC, is it an NK? No, it's an IKDC. *Nat Med.* 2006; 12:167–168. [PubMed: 16462794]
25. Spits H, Lanier LL. Natural killer or dendritic: what's in a name? *Immunity.* 2007; 26:11–16. [PubMed: 17241957]
26. Blasius AL, Barchet W, Cella M, Colonna M. Development and function of murine B220⁺CD11c⁺NK1.1⁺ cells identify them as a subset of NK cells. *J Exp Med.* 2007; 204:2561–2568. [PubMed: 17923504]
27. Endharti AT, Rifa'i M, Shi Z, Fukuoka Y, Nakahara Y, Kawamoto Y, Takeda K, Isobe K, Suzuki H. Cutting edge: CD8⁺CD122⁺ regulatory T cells produce IL-10 to suppress IFN- γ production and proliferation of CD8⁺ T cells. *J Immunol.* 2005; 175:7093–7097. [PubMed: 16301610]
28. Caminschi I, Ahmet F, Heger K, Brady J, Nutt SL, Vremec D, Pietersz S, Lahoud MH, Schofield L, Hansen DS, et al. Putative IKDCs are functionally and developmentally similar to natural killer cells, but not to dendritic cells. *J Exp Med.* 2007; 204:2579–2590. [PubMed: 17923506]
29. Gerosa F, Baldani-Guerra B, Nisii C, Marchesini V, Carra G, Trinchieri G. Reciprocal activating interaction between natural killer cells and dendritic cells. *J Exp Med.* 2002; 195:327–333. [PubMed: 11828007]
30. Steinman RM, Pack M, Inaba K. Dendritic cells in the T-cell areas of lymphoid organs. *Immunol Rev.* 1997; 156:25–37. [PubMed: 9176697]
31. Woodland DL, Dutton RW. Heterogeneity of CD4⁺ and CD8⁺ T cells. *Curr Opin Immunol.* 2003; 15:336–342. [PubMed: 12787761]
32. Moretta L, Ferlazzo G, Bottino C, Vitale M, Pende D, Mingari MC, Moretta A. Effector and regulatory events during natural killer-dendritic cell interactions. *Immunol Rev.* 2006; 214:219–228. [PubMed: 17100887]
33. Sullivan BM, Juedes A, Szabo SJ, von Herrath M, Glimcher LH. Antigen-driven effector CD8 T cell function regulated by T-bet. *Proc Natl Acad Sci USA.* 2003; 100:15818–15823. [PubMed: 14673093]

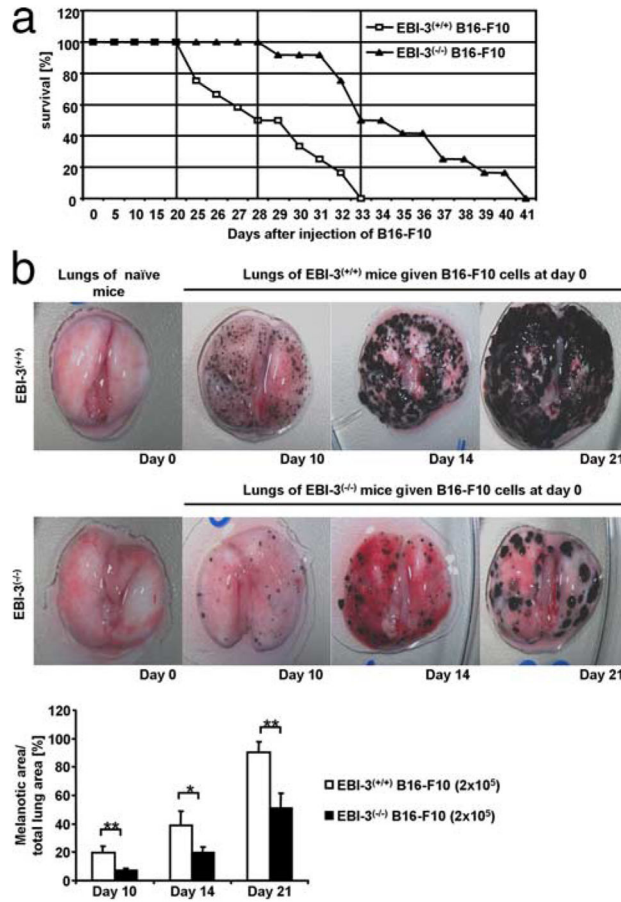


FIGURE 1.

EBI-3-deficiency protects mice from metastases of lung melanoma. *a*, Intravenous injection of the B16-F10 cell line (2×10^5 cells) leads to increased survival of EBI-3^{-/-} lung melanoma-bearing mice ($n = 11$). *b*, Time-dependent development of the melanoma metastases in the lungs of B6 wild-type mice (*upper panels*) as well as in EBI-3^{-/-} lungs (*lower panels*) ($n = 15$). Quantification analysis shows that the area of the lungs covered with melanotic colonies on days 10, 14, and 21 is significantly reduced in EBI-3^{-/-} lungs (*, $p < 0.05$; **, $p < 0.01$). All data represent mean values \pm SEM of three independent experiments.

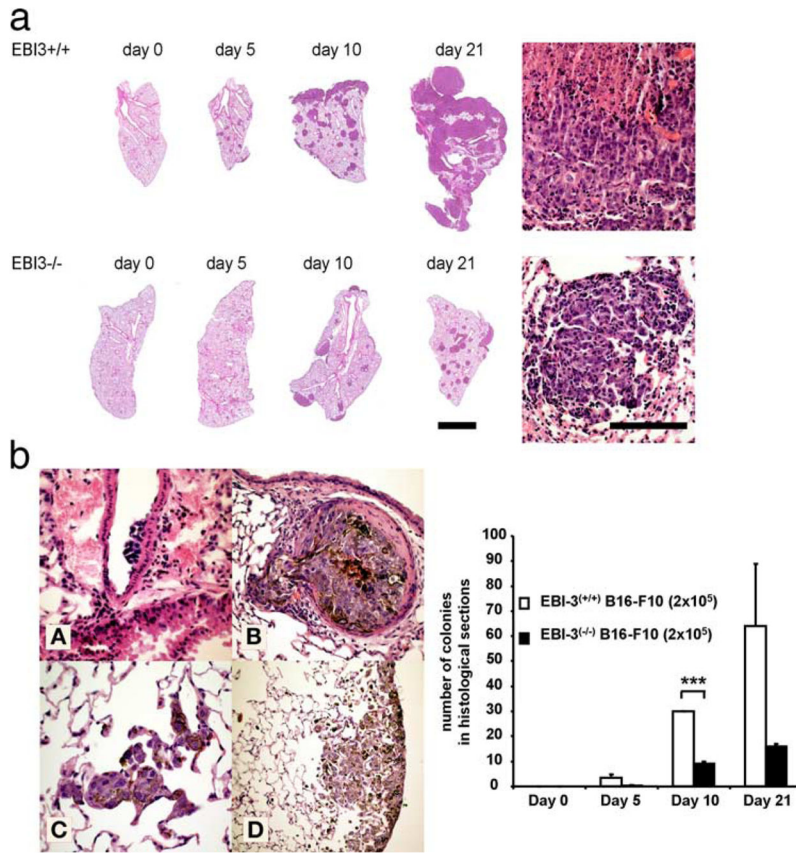


FIGURE 2.

Histopathological analysis of the role of EBI-3 in metastases. *a*, Representative histological sections across lungs of wild-type (*upper images*) and EBI-3^{-/-} mice (*lower images*). Sections were taken at the indicated time points 0, 5, 10, and 21 days after tumor cell injection. The higher magnification images rendered on the right side of the image show representative sections of melanoma metastases. Space bars correspond to 2.5 mm for the histological overviews and 200 μm for the high magnification images on the right (*n* = 5). *b*, *Lower left panels*: A–D, Histological slides showing tumor cells adherent to the endothelium of a large vessel (A), emigration from a vessel filled with tumor cells (B), and tumor cell entry in the lung microvessels (alveolar capillaries) (C). D, Tumor cells adhering to the pleura. *b*, *Lower right panel*, Quantification analysis of histological sections showed a decreased number of melanotic colonies in the tumor bearing lungs of EBI-3^{-/-} mice compared with the wild-type mice (*n* = 5). All data represent mean values ± SEM of three independent experiments (*n* = 5) (*, *p* < 0.05; **, *p* < 0.01; ***, *p* < 0.001).

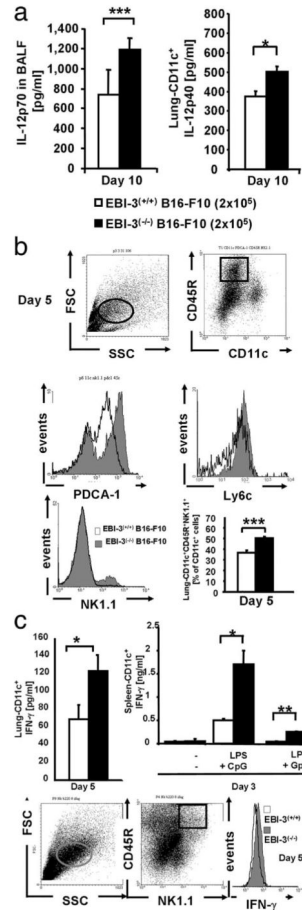


FIGURE 3.

Analysis of immune cells and cytokines in the airways of $EBI-3^{-/-}$ mice developing lung melanoma. *a, Left panel*, Increased IL-12p70 levels were detected in the BALF from $EBI-3^{-/-}$ mice as compared with wild-type mice at day 10 after B16-F10 cell injection. *Right panel*, CD11c⁺ cells were isolated from the lungs of wild-type and $EBI-3^{-/-}$ mice 10 days after i.v. B16-F10 cell injection, and cultured overnight. The supernatant was then collected and analyzed by ELISA for IL-12p40 ($n = 5$). *b*, Increased number of CD11c⁺B220⁺NK1.1⁺ cells in the lungs of $EBI-3$ -deficient mice. Total cell suspensions from the lungs of $EBI-3^{-/-}$ and C57/BL6 wild-type mice were immunostained for the indicated markers and analyzed by FACS. The lung DCs were gated by following previously described methods (*left upper panel*). No significant difference in the total number of lung CD11c⁺ cells was detected (1.860 ± 0.12 for $EBI-3^{+/+}$ vs 2.58 ± 0.004 for $EBI-3^{-/-}$ CD11⁺ lung cells, respectively). The plasmacytoid DCs were identified as CD11c⁺CD45R (B220)⁺PDCA-1⁺ cells (26) (*right upper panel* and *middle left panel*, respectively) were found to be up-regulated in the lungs of $EBI-3$ -deficient mice 5 days after tumor cell injection. Moreover, pDCs are Ly6c⁺. By gating on CD11c⁺B220⁺ cells, we also found increased in CD11c⁺B220⁺Ly6c⁺ in the lung of $EBI-3^{-/-}$ mice. The IK-DC population was up-regulated in the lung of $EBI-3^{-/-}$ mice 5 days after tumor cell injection as compared with wild-type mice (*right lower panel* and *middle right graph*) $n = 5$. *c, Left upper panel*, Supernatants of lung CD11c⁺ cells from $EBI-3^{-/-}$ mice released increased amounts of IFN- γ 5 days after tumor cell injection as compared with those isolated from wild-type littermates. *Lower panels*, CD11c⁺ lung cells from $EBI-3^{-/-}$ and wild-type mice were immunostained for intracellular FACS analysis. On day 5 after tumor cell injection, $EBI-3^{-/-}$ lung cells expressing the markers for IK-DCs produced higher amounts of IFN- γ as compared with the wild-type littermates (*right lower panel*). Splenocytes derived from $EBI-3^{-/-}$ mice that were injected with B16-F10 cells 3 days before released increased amounts of IFN- γ as compared with those isolated from the wild-

type littermates upon 24 h LPS (1 $\mu\text{g/ml}$) and CpG (10 μM) stimulation (*upper right panel*). All data represent mean values \pm SEM of three independent experiments ($n = 5$). (*, $p < 0.05$; **, $p < 0.01$; ***, $p < 0.001$).

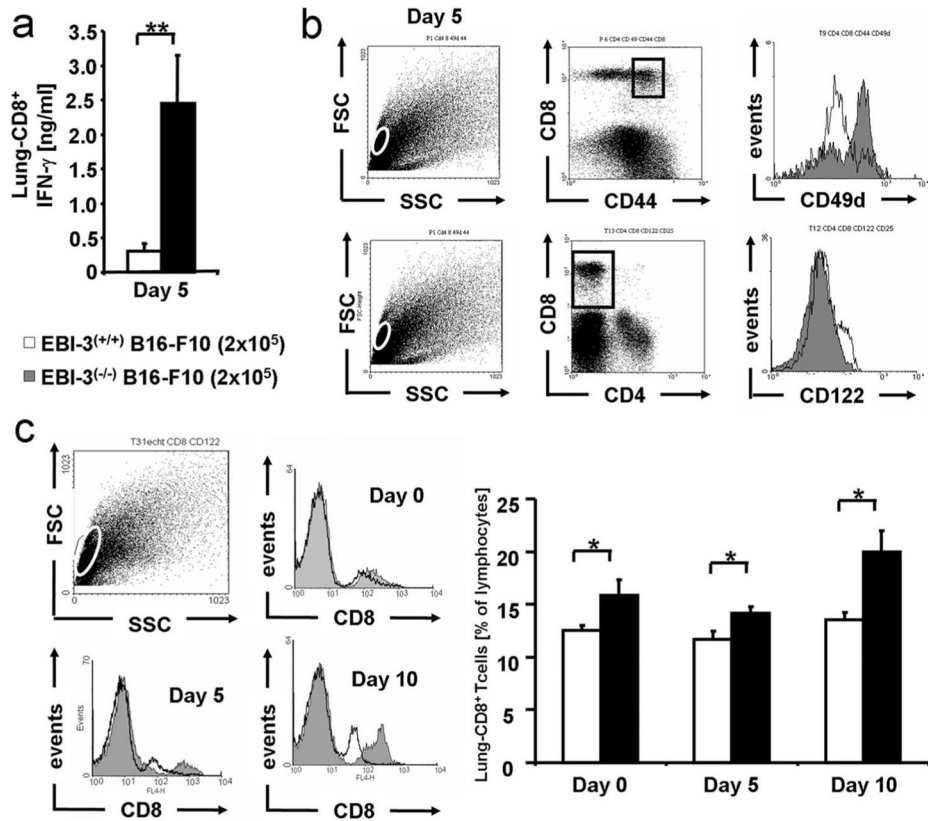


FIGURE 4.

Expansion of activated CD8⁺ T cells releasing IFN- γ in the lungs of EBI-3-deficient mice in a murine model of melanoma. The total number of CD8⁺ T cells isolated from the lungs of EBI-3^{-/-} and wild-type littermates did not differ (4.673 ± 0.63 and 5 ± 0.438 for wild-type and EBI-3^{-/-} respectively). *a*, Lung CD8⁺ T cells from wild-type and EBI-3^{-/-} mice were isolated at day 5 after tumor cell injection. Production of IFN- γ by anti-CD3 Ab stimulated CD8⁺ T cells was measured after 24 h by ELISA. CD8⁺ T cells from EBI-3^{-/-} mice produced significantly (***, $p < 0.001$) higher levels of IFN- γ as compared with wild-type control cells. *b*, Lungs of EBI-3^{-/-} and B6 wild-type mice were stained for the indicated markers and analyzed by FACS (*upper panels*). VLA-4 (CD49d) was found to be significantly increased on activated EBI-3^{-/-} CD8⁺ T cells after B16-F10 cell injection (*lower panels*). Lung CD8⁺CD122⁺ T cells were down-regulated in EBI-3^{-/-} mice 5 days after i.v. injection of the B16-F10 cell line. *c*, Increase of lung CD8⁺ T cells in EBI-3^{-/-} mice during tumor development as compared with wild-type littermates as shown by FACS analysis. All data are representative of three independent experiments (five mice per group).

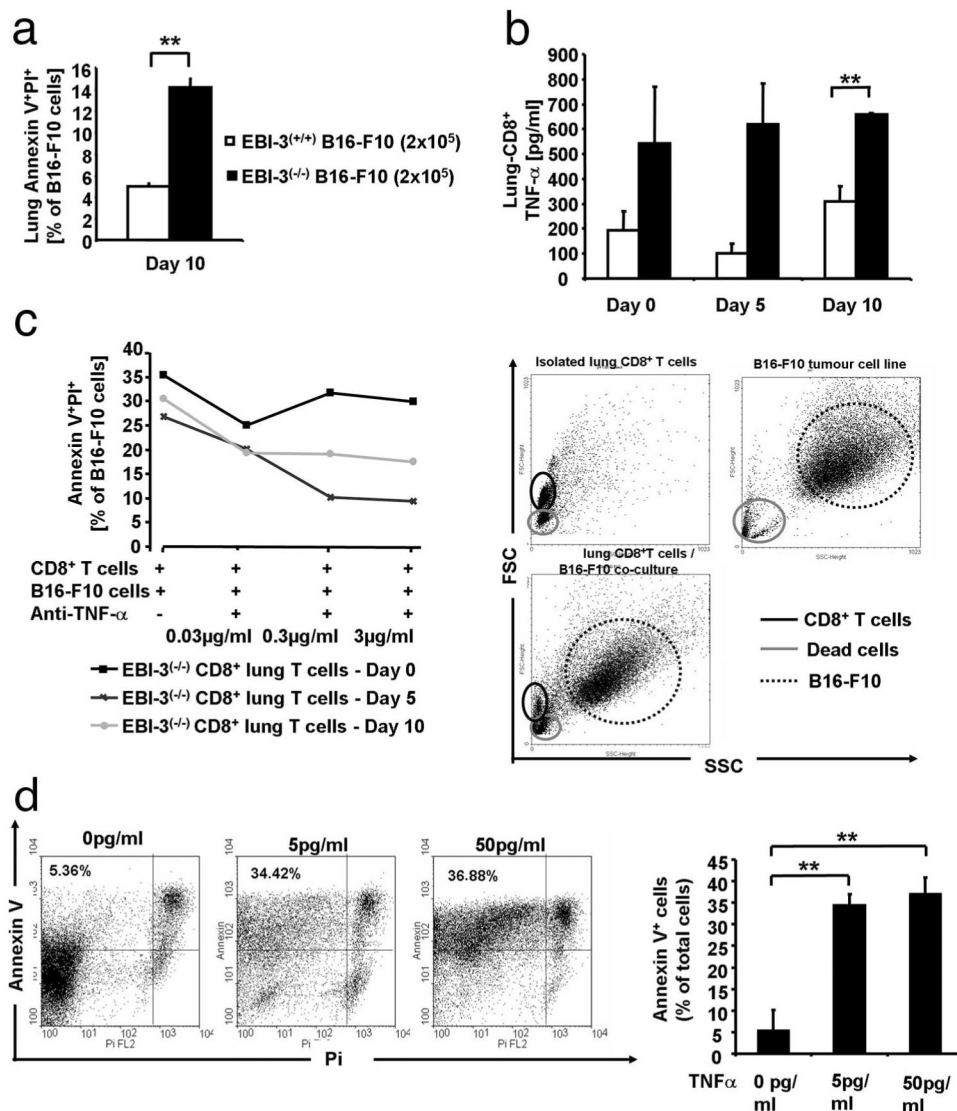


FIGURE 5.

Apoptosis of B16-F10 cells is induced by TNF- α released by CD8⁺ T cells isolated from the lungs of EBI-3 deficient mice. *a*, FACS staining for Annexin V and propidium iodide in total lung cell suspension of tumor bearing mice showed significantly (**, $p < 0.01$) increased apoptosis of B16-F10 cells in EBI-3^{-/-} mice 10 days after i.v. injection of the melanoma cell line ($n = 5$). *b*, Production of TNF- α in 24-h supernatants of lung CD8⁺ T cells was measured by ELISA and found to be significantly (**, $p < 0.01$) increased in EBI-3^{-/-} mice as compared with wild-type mice. *c*, Suppression of apoptosis on target tumor cells was achieved by giving increasing concentration of anti-TNF- α Ab to the coculture of isolated EBI-3^{-/-} lung CD8⁺ T cells with B16-F10 cells ($n = 5$ per group). On the right hand side, a representative dot-plot is shown. *Upper left panel*, Gate on the lymphocytes area excluding the dead cells on the lower left corner. *Upper right panel*, Gate of the B16-F10 is shown on the right-upper corner being distinct from dead cells on the lower left corner. *Lower panel*, Both cell populations are shown. *d*, B16-F10 cell line were cultured overnight with the indicated concentration of recombinant mouse TNF- α . After that, cells were harvested and stained with Annexin V-propidium iodide as described in *Materials and Methods*. Increased Annexin V⁺ cells were observed by increasing the doses of TNF- α . All data are representative of three independent experiments ($n = 5$).

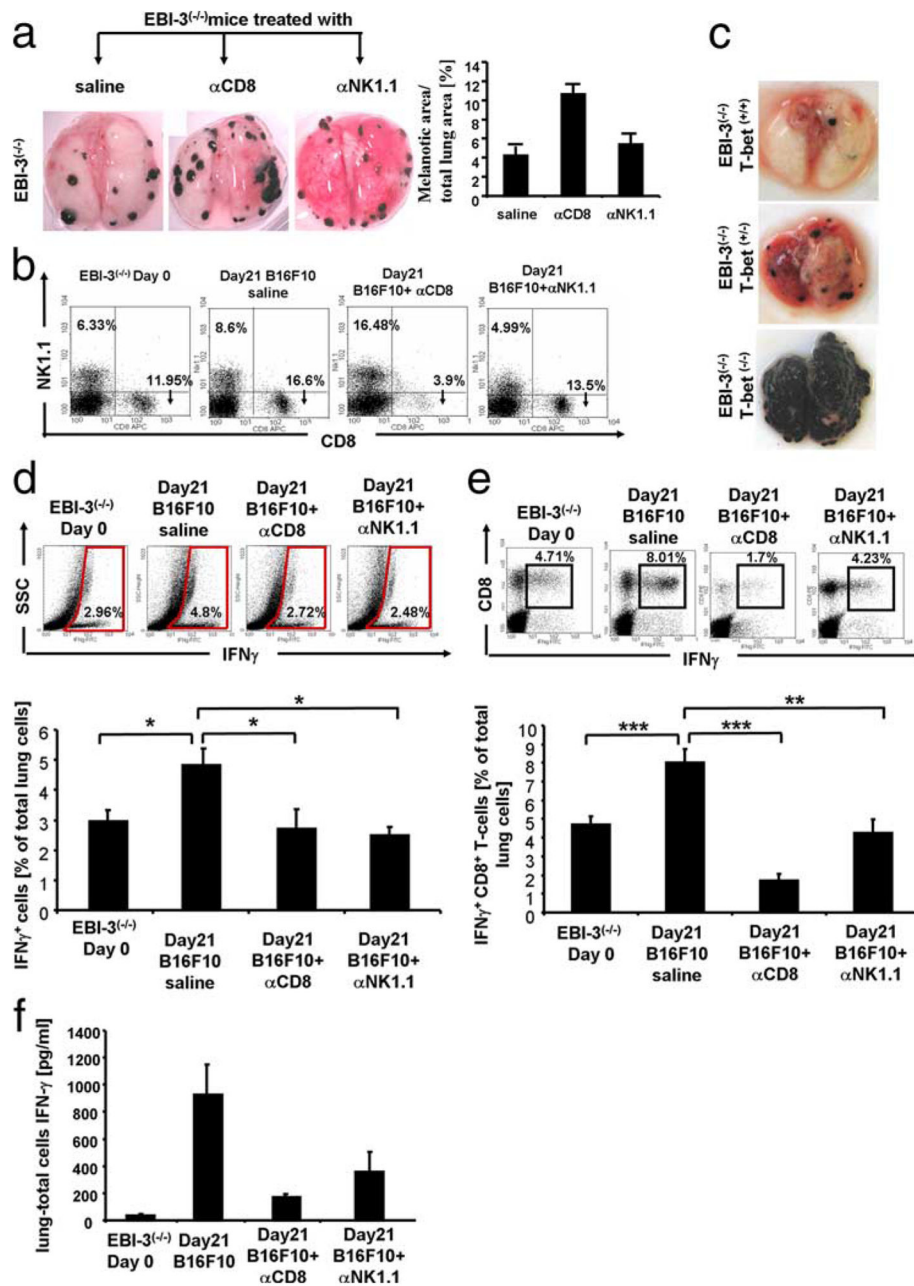


FIGURE 6.

Targeted deletion of T-bet abrogates the protective effect of EB1-3 deficiency on melanoma metastasis. *a*, Five i.p. applications of anti-CD8-induced (250 micrograms/application) lung metastasis in EB1-3^{-/-} mice (*middle panel*) as compared with untreated mice (saline) injected with 2×10^5 B16-F10 18 days before. Anti-NK1.1 (100 micrograms/application) Abs treatment resulted in unchanged tumor load in EB1-3^{-/-} mice bearing tumors (*right panel*) as compared with untreated mice ($n = 4$). *b*, Lung cell suspension obtained from EB1-3^{-/-} mice bearing tumor (Day21, B16-F10) untreated or treated with anti-CD8 and anti-NK1.1 Abs as well as control mice (day 0) were analyzed for CD8⁺ and NK1.1⁺ T cells by FACS analysis. *c*, EB1-3^{-/-} mice on a C57BL6 background were backcrossed with T-bet^{-/-} on the same genetic background for at least ten generations and then analyzed 18 days after B16-F10 cell injection for lung metastases. Targeting T-bet on an EB1-3^{-/-} background resulted in increased tumor load ($n = 4$ per each group). *d*, Anti-CD8 and anti-NK1.1 Abs treatment resulted in decreased intracellular IFN-

γ production in the lung of EBI-3^{-/-} mice 18 days after B16-F10 cells injection. Total lung cells were stained with anti-mouse IFN- γ and analyzed by FACS as described in *Materials and Methods* ($n = 4$) and gating on total lung cells. *e*, Intracellular analysis as in *d* was performed after gating on CD8⁺ T cells. *f*, Total lung cells from EBI-3^{-/-} mice treated in vivo with indicated Abs or untreated were cultured overnight with anti-CD3 and anti-CD28 Abs. The supernatants were collected and analyzed by ELISA for IFN- γ .

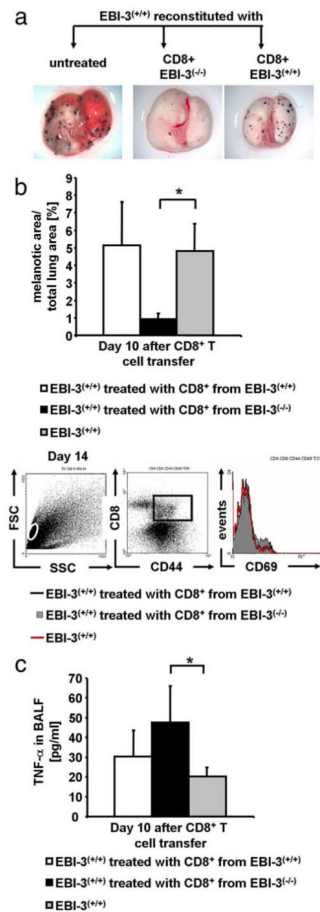


FIGURE 7.

In vivo transfer of CD8⁺ T cells isolated from EBI-3-deficient mice bearing tumor protects wild-type recipient mice from B16-F10 induced lung tumors. *a*, Five $\times 10^5$ tumor Ag primed CD8⁺ lung T cells from both EBI-3^{+/+} (middle lung) and EBI-3^{-/-} (right lung) mice were isolated and together with 2×10^5 B16-F10 cells i.v. transferred into B6 wild-type mice. Untreated tumor-bearing controls received 2×10^5 B16-F10 cells (left lung). Quantification analysis 10 days after the cell transfer showed significantly (*, $p < 0.05$) reduced melanoma growth in the lungs of mice treated with tumor Ag primed CD8⁺ T cells from EBI-3^{-/-} lungs as compared with wild-type controls (*lower panel*). *b*, Staining of total lung cell suspension for CD8⁺, CD44⁺, and CD69⁺ was performed by FACS analysis. An increased number of activated CD8⁺ T cells were observed in recipients of EBI-3^{-/-} CD8⁺ T cells. *c*, The levels of TNF- α in the BALF were measured by ELISA and found to be significantly (*, $p < 0.05$) elevated in mice given EBI-3^{-/-} CD8⁺ T cells as compared with wild-type cells. All data represent mean values \pm SEM of three independent experiments (five mice per group).